



HAL
open science

Towards the Design of Wireless Communicating Reinforced Concrete

Gael Loubet, Alexandru Takacs, Daniela Dragomirescu

► **To cite this version:**

Gael Loubet, Alexandru Takacs, Daniela Dragomirescu. Towards the Design of Wireless Communicating Reinforced Concrete. *IEEE Access*, 2018, 6 (1), pp.75002-75014. 10.1109/ACCESS.2018.2883434 . hal-02067206

HAL Id: hal-02067206

<https://laas.hal.science/hal-02067206v1>

Submitted on 12 Dec 2024

HAL is a multi-disciplinary open access archive for the deposit and dissemination of scientific research documents, whether they are published or not. The documents may come from teaching and research institutions in France or abroad, or from public or private research centers.

L'archive ouverte pluridisciplinaire **HAL**, est destinée au dépôt et à la diffusion de documents scientifiques de niveau recherche, publiés ou non, émanant des établissements d'enseignement et de recherche français ou étrangers, des laboratoires publics ou privés.



Distributed under a Creative Commons Attribution 4.0 International License

Date of publication xxxx 00, 0000, date of current version xxxx 00, 0000.

Digital Object Identifier 10.1109/ACCESS.2017.Doi Number

Towards the Design of Wireless Communicating Reinforced Concrete

Gaël Loubet¹, Alexandru Takacs^{1, 2}, Member, IEEE, and Daniela Dragomirescu^{1, 3}, Senior Member, IEEE

¹Laboratory for Analysis and Architecture of Systems (LAAS), National Center for Scientific Research (CNRS), Toulouse, F-31031 France.

²University Paul Sabatier (UPS), University of Toulouse, Toulouse, F-31062 France.

³National Institute of Applied Sciences (INSA) of Toulouse, Toulouse, F-31077, France.

Corresponding author: Gaël Loubet (e-mail: gael.loubet@laas.fr).

This work was supported in part by the French National Research Agency (ANR) under the McBIM project (Communicating Material at the disposal of the Building Information Modeling), ANR-17-CE10-0014.

ABSTRACT This paper addresses the concept of a smart-node wireless network designed for structural health monitoring applications. The network architecture is based on a smart mesh composed of sensing nodes and communicating nodes. The sensing nodes are used to implement the so named communicating material/communicating concrete and collect physical data for structural health monitoring purposes. These data are sent to the communicating nodes that interface the smart-node network with the digital world through the Internet. The sensing nodes are batteryless and wirelessly powered by the communicating nodes *via* a wireless power transmission interface. Experimental results have been obtained for a simplified sensing node using a LoRaWAN uplink wireless communication (from the sensing node to the communicating node) proving that the functionality of the sensing nodes can be controlled wirelessly by using only the wireless power transmission downlink.

INDEX TERMS Communicating Materials, Wireless Power Transmission (WPT), Wireless Sensor Network (WSN).

I. INTRODUCTION

The emerging of Internet of Things (IoT) technologies has generated many new possibilities in the field of Structural Health Monitoring (SHM) of buildings and civil and transportation infrastructures (e.g. railway and subway stations, bridges, highways, etc.). Also, the structural health monitoring of buildings, through innovative IoT technologies and approaches, is part of the Smart City concepts and paradigms. Recently, the Building Information Modeling (BIM) concept [1] has provided new tools to more efficiently plan, design, construct, and manage buildings and infrastructures.

An innovative approach to implement the SHM and BIM concepts for construction, civil and transportation engineering is the use of the so named ‘communicating material’ [2]. The research project McBIM [3] - Communicating Material at the disposal of the Building Information Modeling- aims to provide a practical application of the concept of communicating material in the construction domain, namely communicating precast reinforced concrete. This will be intrinsically able to

generate, process, store and exchange data over several meters or more from its environment and internal physical states to dedicated system(s) -in particular a virtual model: the BIM-, with the ability to function for several decades.

A few works have already provided implementations of communicating materials based on Radio Frequency Identification (RFID) for various materials and aims. Among them can be found the storage and access at short range of some disseminated data in wood [4], textile [5], and concrete [6].

Reinforced concrete is the most common construction material thanks to its scalability, durability and cost [7]. Three particular stages of its life cycle are targeted: the manufacture and storage of precast elements, the construction of a structure, and the exploitation of these construction works, particularly through structural health monitoring. The works [6], [8], [9], and [10] suggest incomplete solutions for the three targeted applications by the project. To implement the ‘communicating concrete’ concept we propose here a smart wireless micro-nodes network able to sense, store, and communicate data; autonomous in terms

of energy; resilient; and connectable to a digital model. The issues concerning installation and maintenance costs are considered, as well as the need of a system that can reliably function for decades.

In Section II of this paper, we will succinctly introduce the envisaged architecture for the wireless micro-nodes network, as well as describing each of its components, namely the communicating (CN) and sensing nodes (SN). The sensing nodes are intended to be embedded in concrete and operate for decades, without any maintenance. Thus, a batteryless approach by using a Wireless Power Transfer (WPT) interface is proposed in order to increase the lifetime and to avoid the maintenance issue. Preliminary results concerning our first prototype of the sensing node, which communicates through the LoRaWAN protocol, are presented in Section III. SN is wirelessly supplied and an innovative and original concept is proposed in Section IV: to control the periodicity of communication - to control the periodicity of communications -and eventually measurements- by using a well-defined and tailored wireless power transfer system. The inherent constraints of the proposed concept as well as the potential improvements are discussed in Section V.

II. WIRELESS NETWORK ARCHITECTURE FOR COMMUNICATING CONCRETE AND MATERIALS

A. ARCHITECTURE OF THE WIRELESS SMART-NODE NETWORK

In order to implement a communicating concrete, a wireless smart-nodes network is set-up by embedding interconnected SNs and CNs into precast reinforced concrete elements.

Each concrete element hosts one or two communicating nodes -located at the concrete/air interface-, and several sensing ones -randomly located in the concrete-, as presented in Fig. 1. Their number will be a function of the physical properties of the concrete element and of an adopted scenario (defined by the end-user). The communication between the SNs and CNs can be made through the concrete (in the case of neighboring SNs and CNs, i.e. embedded in the same concrete element) or across the air or by all combination of air and concrete as a function of the relative positions of the SNs and CNs. As detailed in the next section, SNs should be low power and batteryless whilst being inaccessible for maintenance whereas CNs will be connected to an energy source (wired electric grid or a high capacitance battery) and accessible for maintenance. The storage of data -in each element and for the entire building- must be redundant, globalized, and secured. For each construction, one or more access points to the digital world -especially to communicate with the BIM- will be available and reprogrammable in order to meet the needs of each stages of the life cycle of the communicating concrete. The term ‘real world’ is used here to describe the communications and the interactions between SNs and CNs or between various CNs on a physical level (i.e. between the nodes located in neighboring concrete

elements belonging to the same building or civil infrastructure) whereas the term ‘digital world’ denotes the data exchange performed on the Internet. The proposed wireless smart-node network acts on a ‘real word’ to collect data and physical measurements and send those data to the digital world where the data are analyzed, stored and used for various (end-user defined) purposes.

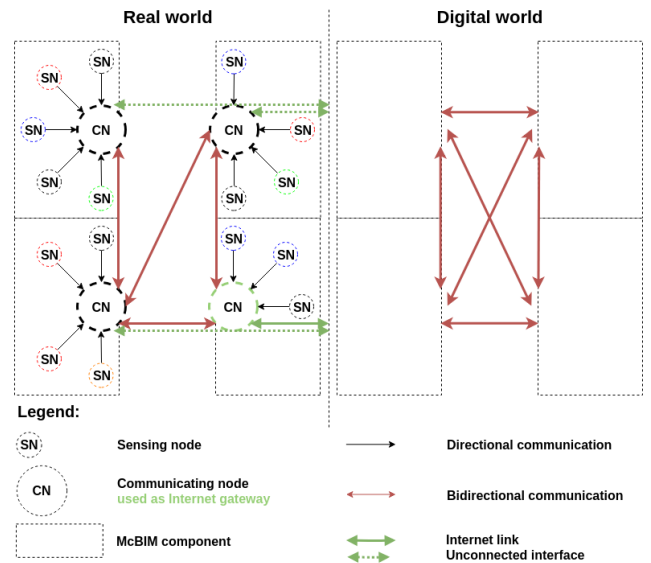


FIGURE 1. Schematic diagram for the envisaged architecture of the smart-nodes network embedded in the precast reinforced concrete.

B. TOPOLOGY OF COMMUNICATING NODES

The topology of communicating nodes is presented in Fig. 2. CNs will securely aggregate, store and share data from sensing nodes, to (and from) other communicating nodes. The data will be collected and shared wirelessly by a radiofrequency transmission across concrete and/or air. In addition, several CNs must implement the communication between *real* and *digital* worlds through a ‘n-G’ cellular network interface (today the ‘3G’ cellular network standard is supported worldwide, ‘4G’ is available in developed countries mainly in the urban regions, while ‘5G’ is under development or implementation). The minimum communication range between SN and CN is in the range of a few meters whereas the communication range between CNs is intended to be much larger (10 to 100 meters or even more). Communicating nodes must follow an energy efficient strategy and be reprogrammable in terms of communication interfaces, and software application. These nodes can be supplied with batteries until the exploitation phase of the building, where they can be switched to their main supply source, if available. Moreover, CNs must wirelessly power the SNs by using a wireless power transfer approach.

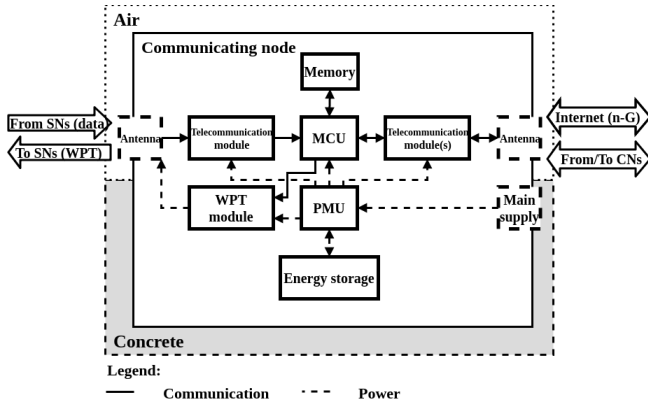


FIGURE 2. Schematic diagram for the envisaged architecture of the communicating nodes.

C. TOPOLOGY OF SENSING NODES

The sensing nodes -presented in Fig. 3- have to generate data by sensing environmental and structural properties of the concrete element (e.g. temperature, humidity, corrosion, cracks detection and location, etc.), and need to transmit these collected data to the associated communicating node(s) through a radiofrequency communication across concrete and/or air. In order to increase the lifetime and to avoid maintenance issues (SNs are embedded in the concrete), the nodes must be autonomous in terms of energy and batteryless. This is feasible by using a wireless power transfer system, managed by the communicating nodes. Moreover, some other restrictions apply for SNs: (i) the overall architecture of a SN needs to be as simple as possible and low power in order to relax the constraints for the WPT interface, (ii) the communication between SNs and CNs is unidirectional (SNs send data to CNs but only receive power *via* the WPT interface), (iii) the embedded intelligence of SNs is quite limited, their complete functionality must be set before embedding the SNs in the concrete, (iv) no reconfigurability is allowed with only a few exceptions that are detailed in this paper. CNs receive data and send power to SNs by using a WPT approach. By modulating the total amount of power transferred to SNs, the CNs can: (i) wirelessly switch on and switch off the SNs, (ii) manage the periodicity of measurement and transmission of the associated sensing nodes. Ideally, no data are stored in the SNs. In a same way, limited processing capabilities (e.g. a microcontroller unit (MCU) that is represented as optional block in Fig. 3) are embedded into the SNs. We target here a generic platform on which we can associate a specific sensor, and with only a simplified physical interface between the sensor and the transmitter. The sensor itself should be capable of performing measurements in a continuous way as long as the SN is switched on. The measured quantities (data) are sent by the SN to the CN as soon as the transmitter of the SN has enough power to perform a transmission slot. Thus, the overall functionality (and partially the reconfigurability) of the SN can be controlled by CNs *via* the WPT interface. To the best of the author's knowledge this innovative concept

has not been reported previously and is considered state-of-the-art. We also note that the capabilities of the WPT interface is limited today mainly by regulations (i.e. the maximum Effective Isotropic Radiated Power (EIRP) that can be radiated by CN is regulated for the ISM bands [40]) and not by the technology itself.

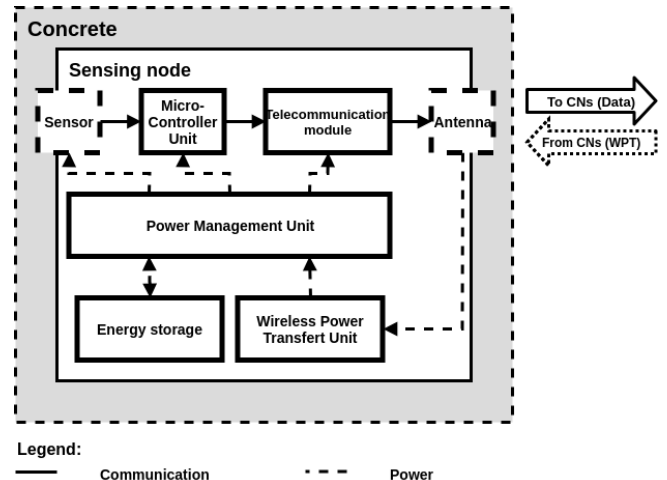


FIGURE 3. Schematic diagram for the envisaged architecture of the sensing nodes.

III. DESIGN OF SENSING NODES

Our first prototype of the sensing node, designed as a proof-of-concept of the adopted architecture, implements several functionalities: (i) the autonomy in terms of energy is assured by the WPT interface, energy storage and power management unit, (ii) a wireless unidirectional communication following LoRaWAN standard was adopted in this work for proof-of-concept purposes, (iii) the periodicity of the communication frames/measurements can be controlled and tuned by CNs *via* the WPT interface. The measurement functionality was not implemented yet in the SN prototype.

A. WIRELESS POWER INTERFACE

One of the main constraints for implementing the SN concerns its energy autonomy. Some recent works [11] reviewed the available energy in buildings and the best strategy to harvest some of this energy. Nevertheless, the ambient sources of energy seem to be too low, too fluctuating and sometimes unavailable in order to operate efficiently for decades. Neither light, nor temperature gradients are available in concrete and the natural resonant frequency of buildings is less than one Hertz making the harvesting of light, thermic or vibrational energy impractical. In our case, radiofrequency wireless power transfer is a convenient solution when well-adapted [12], [13]. The main advantage of WPT is the control of the whole transmission chain. The user can control the frequency and the amount of transmitted power, therefore the system efficiency can be accurately estimated for a given scenario [12]. Unlike [14], [15], and [16] which work on magnetic WPT, the far-field WPT is

more relevant in our case because of the targeted distance between the sensing and communicating nodes. This distance is in the range of a few to tens of meters, with the possibility of even more if an appropriate frequency band is selected (e.g. ISM 868/915 MHz). The wireless power interface consists of a high-frequency rectifier connected to a WPT receiving antenna, forming a rectenna (acronym from *rectifying antenna*). The WPT antenna captures the ambient electromagnetic energy and converts it into a RF signal. The rectifier converts the guided RF signal into the DC power for supplying the Power Management Unit (PMU). This PMU contains a DC-to-DC boost convertor that charges a storage energy element (e.g. supercapacitors). The energy stored in the storage element is then used by the PMU to power the SN electronics: the sensor, the low power MCU (if used, the MCU is not mandatory), and the telecommunication module (a low power transmitter in our case). The largest amount of DC power is required by the transmitter (Tx) device during the transmitting of data collected from the sensor(s). Hopefully in most of these scenarios, the measurements will not need to be performed continuously (e.g. the temperature and the humidity should be measured every hour, etc.).

The adopted topology for rectenna design is represented in Fig. 4. The key component of the WPT interface (rectenna) is the non-linear device (e.g., Schottky diode or transistor) used to convert the RF signal into a DC voltage. This device is carefully selected for rectifying low-power signals. Moreover, the rectifying process generates undesirable harmonics at the input and output ports of the non-linear device. At the input port of the non-linear element/rectifier, a matching circuit acting as a band-pass filter is used to prevent these harmonics from being re-radiated by the antenna and to maximize the power conversion efficiency. The harmonics generated at the output port of the non-linear device are filtered by a low-pass filter. The load (that is the PMU of SN) is then supplied with the required DC power to operate.

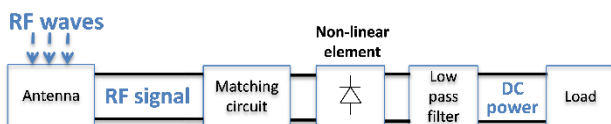


FIGURE 4. Rectenna topology.

We used a rectenna previously developed in our laboratory [17], [18]. It is composed of a compact and broadband flat dipole antenna (enclosed by a rectangular ring) and a single diode rectifier orthogonally connected with the antenna as shown in Fig. 5. The antenna was manufactured on a FR4 substrate (substrate thickness: 0.8 mm, relative electric permittivity: 4.4 and loss tangent: 0.02) whereas the rectifier was manufactured on Rogers RT/Duroid 5870 substrate (substrate thickness: 0.787 mm, relative electric permittivity: 2.3 and loss tangent: 0.0012). The selected Schottky diode (Avago HSMS 2850) is serially connected with the matching circuit and the load. The impedance matching circuit is composed of a bent short-circuited stub and a 30nH inductor

for matching the input impedance of the rectifier around 900 MHz. More details concerning the design and the characterization of the rectenna are reported in [17], [18]. Fig. 5 shows a photo of the manufactured rectenna with its main dimensions. The results depicted in Fig. 6 demonstrate that the manufactured rectenna operates efficiently for low power densities of the incident RF waves: a DC power greater than $20\mu\text{W}$ can be harvested as long as the incident power density exceeds $0.4\mu\text{W}/\text{cm}^2$. Moreover, this rectenna is relatively broadband, covering ISM 868/915MHz frequency band and part of the GSM bands.

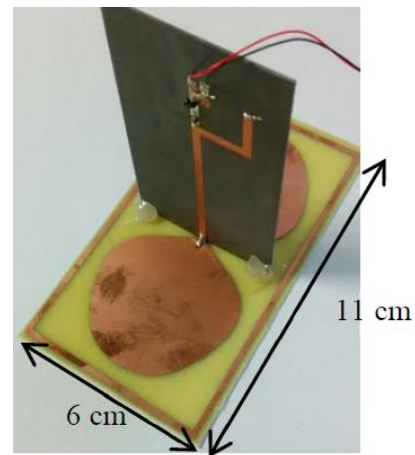


FIGURE 5. Photograph of the manufactured rectenna.

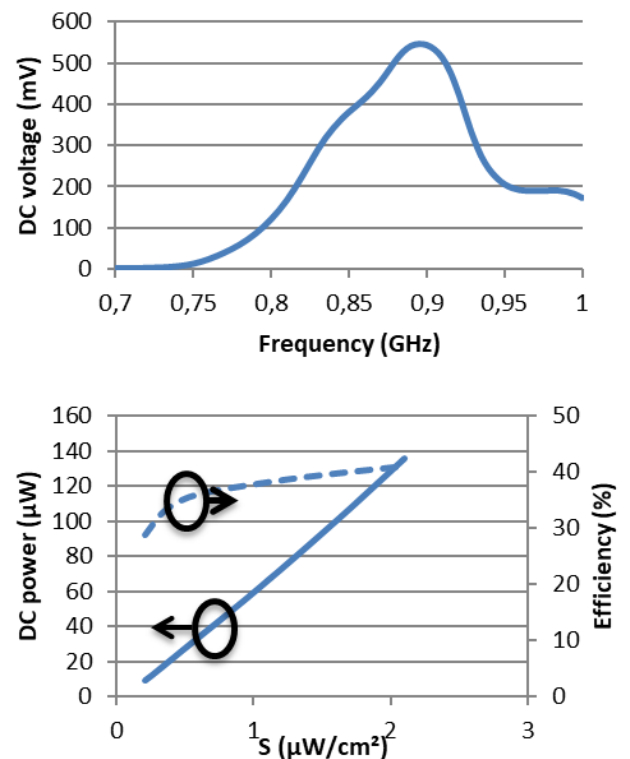


FIGURE 6. Rectenna performances measured on a resistive load of 10 k Ω : a) DC voltage as function of frequency, b) DC power and power conversion efficiency as function of the illuminating/incident power densities (frequency: 900 MHz).

wireless communication technologies is displayed in Table I. For the communication between SNs and CNs we only need a unidirectional uplink communication over a few or tens of meters. In the majority of presented standards, bidirectionality is the norm. Nevertheless, LoRaWAN and Bluetooth Low Energy (BLE) can be used only for transmitting data and consequently, control frames (e.g. acknowledgement frames) are not needed. The protocol constraints (e.g. control frames or duration of a transmission) for the selected wireless technology must be considered in order to estimate the energy consumption and thus calibrate the energy storage element. According to Table I, the BLE module is more suitable for our application, in the case of a broadcaster/observer topology, i.e. without connection. Although no module is available, the RuBee standard could be a real opportunity for the McBIM project too. Indeed, reinforced concrete is composed -among others- with multiple materials consisting of different grain sizes, but these sizes are very small when compared with the wavelength at 131 kHz (i.e. 2288 meters in free space). Also, the concrete seems to be transparent for the magnetic field propagation (RuBee operates in near field, with the magnetic field as communication vector) at such a low frequency (131 kHz).

Regarding the prototype, the sent messages are received by a LoRa gateway installed on INSA campus (Toulouse, France, GPS coordinates: 43°34'14.8"N 1°27'58.5"E); at a distance of more than one kilometer from our workspace (LAAS-CNRS Toulouse, France, GPS coordinates: 43°33'45.3"N 1°28'38.4"E). The data are then transmitted to the TheThingsNetwork [29] network, where we can recover and process them.

The communication part is as simplified as possible. We embedded a simple processing system in the sensing node. Thus, a byte of data (hard coded now, but in the future provided by a sensor) is transmitted each time when the system is supplied. The length of the transmitted frame is set at 14 bytes (there are 13 bytes dedicated to the protocol in a LoRaWAN frame and 1 byte of data). The transmission respects LoRaWAN class A standards (the node sends data but it cannot be interrogated), with a +2dBm radio frequency output power at 868MHz (ISM band), an activation by personalization (ABP), and without causing an acknowledgment from the network. This all aids to limit the number of exchanges, and reduce power consumption. The bandwidth is 125kHz, and the spreading factor is 12, allowing a data-rate of 293bps. The transmission time estimated by the LoRa module is 1.156s. Specifically, the software initializes the MCU, the useful peripherals, and the SX1276 module, then makes a LoRaWAN transmission, before being deactivated and shifting to a deep-sleep mode. Fig. 9 provides a consumption profile for the B-L072Z-LRWAN1 board. The treatment lasts approximately 1.4s (0.25s for the initialization and 1.15s for the transmission). The system needs at least 150mJ to work properly, as

detailed later. The software is limited to a low applicative program, the LoRaWAN stack, and several drivers. The recovering, processing and storing of data on the servers has not yet been implemented. We only visually checked on a web-browser for good reception of data as presented in Fig. 10. In this figure, we can validate the good transmission of two frames providing the same data: '5A' in hexadecimal (or '01011010' in binary); with 2h 59min 16s between each one. Other indicators are available as device information (time of reception, frame index, etc.), LoRaWAN parameters (central frequency, kind of physic modulation, data-rate, coding-rate, etc.), and reception indicators (gateway ID, RSSI, SNR, etc.).

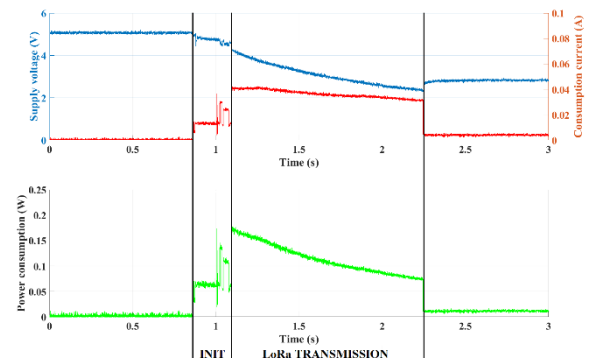


FIGURE 9. Consumption profile of the B-L072Z-LRWAN1 board connected to the PMU and rectenna when a 30mF capacitance charged at 5.15V is used as storage element.

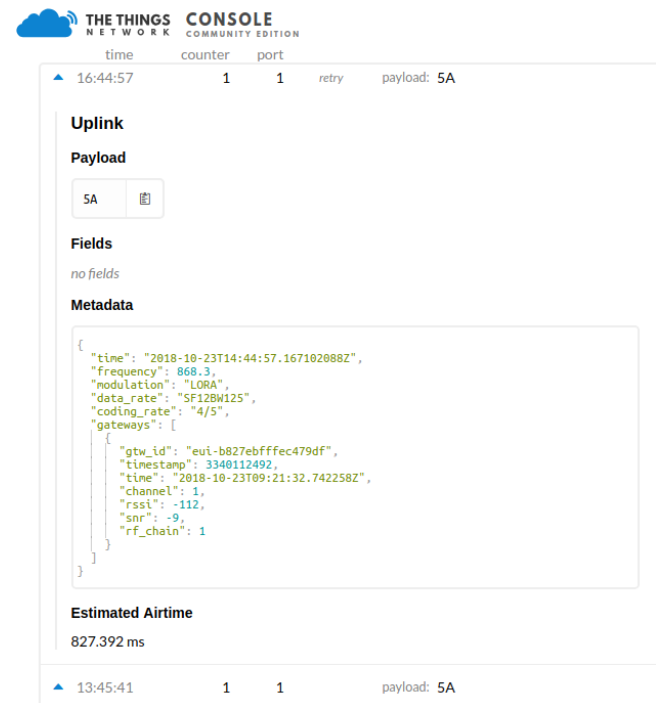


FIGURE 10. Screenshot of TheThingsNetwork interface after receiving checked frames, when the SN was illuminated with a power density of 1.12μW/cm² through the WPT interface.

IV. EXPERIMENTAL RESULTS

Our experiments were carried out in three main steps. Firstly, we characterized our prototype with a controlled input power. Secondly, we tested our system with the rectenna and a RF power transmitter in an anechoic chamber. Finally, we tested our system in a real outdoor environment in order to create easier communication with the LoRaWAN gateway.

A. COMPLETE PROTOTYPE SPECIFICATIONS

Our prototype, developed as a proof of concept in this paper is composed of: (i) a B-L072Z-LRWAN1 board used as a wireless telecommunication unit (ii) a bq25504 used as PMU and connected with KEMET supercapacitors used as storage elements (iii) a rectenna [18] used as WPT interface -this rectenna was designed and optimized for ISM 915 MHz (USA) frequency band but it can be used also in the ISM 868 MHz (EU) frequency band, as presented in Fig. 6-.

The B-L072Z-LRWAN1 board consumes on average 107.3mW, i.e. 32.9mA at 3.36V (average value from 5.15V to 2.45V), during 1.4s, (measured and computed from Fig. 9). Consequently, a minimum energy of 150mJ is needed to execute all the steps required by a complete LoRaWAN transmission. In our tests we used a capacitance of nearly 30mF in order to anticipate the energy consumption for measurement (our prototype does not yet integrate the sensor) and to have a margin for unexpected losses. The energy stored (E) by the storage element can be estimated as:

$$E = \frac{C}{2} \cdot (V_{max}^2 - V_{min}^2) \quad (1)$$

where C is the capacitance of the energy storage element, V_{max} and V_{min} the maximal and minimal voltages at the ports of the storage element defined thanks to the bq25504 configuration pins (respectively OK_HYST -pin number 9- and OK_PROG -pin number 10-). Thus, for C=30mF, we obtain:

$$E = \frac{30 \cdot 10^{-3}}{2} \cdot (5.15^2 - 2.45^2) = 308mJ \quad (2)$$

The energy stored (estimated at 308mJ by using theoretical computation) in the storage element (30mF) is sufficiently higher than the needed 150mJ. Although it is not the optimal solution, to approximate this value we used an array of three FM0H103ZF 10mF supercapacitors in parallel.

B. EXPERIMENTATIONS WITH CONTROLLED INPUT POWER

For our first test, we connected directly the RF signal generator (Anritsu MG3694B) with a rectifier (available in our laboratory, this rectifier is a 'precursor' of the rectifier integrated in our 3D rectenna but operates around 985MHz due to its different/not optimized matching circuit). Our system is efficient from -4dBm of RF power at the input of the rectifier, -providing nearly 350mV, enough to start-up (switch-on) the PMU-. Once started, the PMU charges efficiently the energy storage element, and we can decrease the input power to below -7dBm. Fig. 11 shows the voltage at the terminals of the energy storage element (an array of

three FM0H103ZF supercapacitors in parallel) for a particular application, i.e. the transmission of LoRaWAN frames as soon as possible with the lowest input RF power. We observed that every 16 seconds there was an increase in the rectifier output voltage which is due to the MPPT process of the PMU, which opens its input to buffer the input voltage and optimize its performance. Table II displays some characteristics of our system for different input powers and for particular transmission frequencies.

$T_{cold\ start}$ corresponds to the cold start period, after which the PMU works with a nominal behavior. The first charge, which is the worst-case scenario, ends after a time of T_{first} . For each discharge the energy stored is consumed by the communication system during $T_{discharge}$. Experimentally, if $T_{discharge}$ is less than approximately 1.4 seconds, the LoRaWAN frame is erroneous or not completely sent. In fact, we need nearly 0.25 seconds to initialize the systems, and 1.15 seconds to transmit a frame with one byte of data. If we do not stop the input power, only a period T_{inter} is needed to have a new transmission.

Thus we are able to modulate the frequency of transmission -and in the future, of the measurement-, without the help of the embedded intelligence -i.e. the MCU-, but due to the control of the transmitted power, which we can modulate in terms of power (at least -4dBm at the input of the rectifier is needed for the cold start, and below -7dBm in the nominal mode), or in terms of periods of transmission. During these experiments, we can impose a period of transmission between 1 minute 09 seconds and 26 minutes, for an input power between -7dBm and +10dBm. It should be noted that the auto-discharge is relatively low, so a complete charge is not necessary each time, if the periodicity of transmission is not too large.

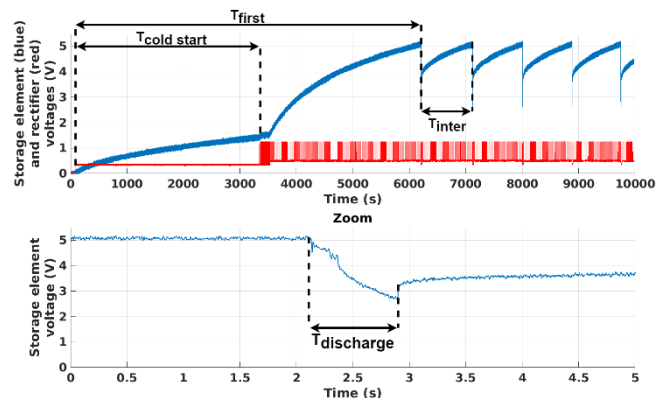


FIGURE 11. a) Evolution of the voltage waveforms at the output ports of the energy storage element (blue) and rectifier output voltage (red) b) Zoom on the voltage at the output ports of the energy storage element during discharge.

C. EXPERIMENTAL RESULTS IN A CONTROLLED ENVIRONMENT: SENSOR NODE POWERED BY A WIRELESS POWER TRANSMISSION TECHNIQUE

The SN prototype was characterized in an anechoic chamber (no multipath or interference effects). As presented in Fig. 12, our system is composed of: (i) a power transmitter (power synthesizer Anritsu MG3694B connected to a patch antenna with a +9.2dBi gain) operating at 868MHz -i.e. in the same ISM band as for the LoRaWAN transmission-, (ii) a 3D rectenna covering booth ISM 868MHz and ISM 915MHz frequency bands, (iii) the PMU (bq25504) and the storage element (30mF -an array of three FM0H103ZF supercapacitors connected in parallel-), (iv) the LoRaWAN board (B-L072Z-LRWAN1), and, (v) an oscilloscope to make voltage waveform measurements (LeCroy WaveRunner 6100). In order to discriminate WPT and communications -which both operate at the same frequency-, and to avoid eventual interferences, we used orthogonal polarizations: the antennas dedicated to the WPT are horizontally polarized, whereas the antenna for the communication is vertically polarized.

We measured some specific cases which are summarized in Table III. The RF power density S (3) is computed as a function of the electric field E (4) (effective value) at the antenna location as:

$$S = \frac{E^2}{120 \cdot \pi} \quad (\text{W/m}^2) \quad (3)$$

with

$$E = \frac{\sqrt{30 \cdot P_T \cdot G_T}}{d} = \frac{\sqrt{30 \cdot \text{EIRP}}}{d} \quad (\text{V/m}) \quad (4)$$

where P_T is the power generated by the RF power synthesizer, G_T the transmission antenna gain, and d the distance between the power transmitter and the rectenna acting as WPT interface for our SN prototype.

The RF power (5) collected by the rectenna can be computed as:

$$P_{RF} = A_{eff} \cdot S \quad (\text{W}) \quad (5)$$

where A_{eff} is the equivalent area of the antenna (6) computed as:

$$A_{eff} = G_R \cdot \frac{\lambda^2}{4 \cdot \pi} \quad (\text{m}^2) \quad (6)$$

where G_R is the rectenna gain and λ the wavelength.

According to (3) and (4), we can generate a power density of $1\mu\text{W}/\text{cm}^2$ at 399cm away from a +33dBm EIRP source.

As we test our system in an anechoic chamber, we cannot validate the transmission of the LoRaWAN frame. Nevertheless, the LoRa transmitter was powered for the duration needed to accomplish all the application software and the transmitted frequency spectrum was displayed through a vector analyzer placed in the anechoic chamber.

Previously, we were able to modulate the period of LoRa transmission by controlling the EIRP of the RF source. In our experiments, the period between two consecutive LoRa transmissions was modulated between nearly 20 minutes

(EIRP=30.7dBm, $d=150\text{cm}$, $S=4.16\mu\text{W}/\text{cm}^2$) and 1 hour and 32 minutes (EIRP=26.7dBm, $d=150\text{cm}$, $S=1.65\mu\text{W}/\text{cm}^2$).

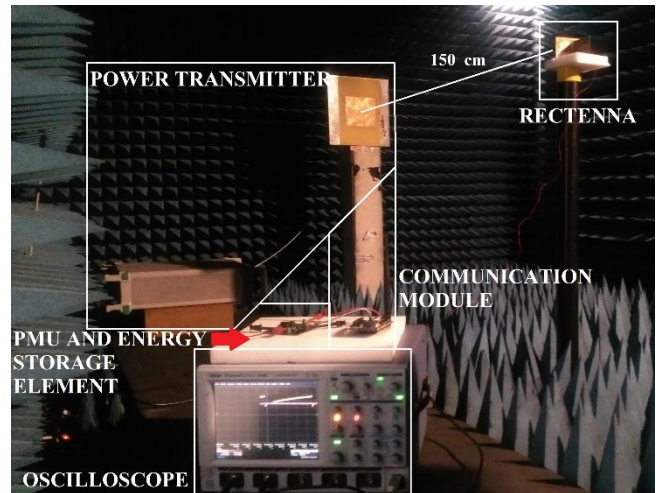


FIGURE 12. Photograph of our experimental setup (SN powered by using a WPT technique) in an anechoic chamber.

D. EXPERIMENTAL RESULTS IN A REAL ENVIRONMENT: SENSOR NODE POWERED BY A WIRELESS POWER TRANSMISSION TECHNIQUE

In order to validate the LoRaWAN transmission, the experimental setup (previously located in anechoic chamber) was installed in a place where we can contact the LoRa gateway more easily (located at the INSA campus, Toulouse, France). The setup is presented in Fig. 13. A power transmitter composed of a signal generator (Anritsu MG3694B), operating at 868MHz, and a patch antenna with +9.2dBi of gain is used as the power source for generating the electromagnetic power density that illuminates the prototype under test. The total losses of the cable and connectors used to interconnect the power generator with patch antenna were approximately -1dB. The measurements were performed on the balcony of our laboratory to ensure the path of least hindrance to the LoRa gateway (located at INSA Toulouse, France) and to be confronted with real environmental conditions (with electromagnetic fields, sun, temperature and humidity variations, wind, etc.) -but not similar to the conditions met inside concrete-. The voltage measurements were performed by using a LeCroy WaveRunner 6100 oscilloscope. The distance between the power transmitter and the rectenna was 150cm or 100cm (in the far field region of the transmitting antenna of the RF source).

In order to discriminate power and communication waves using the same frequency; we chose to use orthogonal polarizations for the WPT and communication (LoRa) links. Thus, the LoRa transmitter and gateway are vertically polarized, whereas the rectenna and power transmitter are horizontally polarized. In this way, no interferences were observed.

As represented in Fig. 14, the energy storage element is charged to 5.15V and discharged to 2.45V. The inter-

discharge time can be modulated by controlling the EIRP of the RF source, as previously demonstrated in the controlled environment (anechoic chamber). We have the possibility to transmit a data frame with a period between 4 minutes and 3 hours. Table IV agglomerates some obtained results for density powers between approximately $1\mu\text{W}/\text{cm}^2$ and $13\mu\text{W}/\text{cm}^2$. Concerning the DC voltage measured at the output ports of the rectenna, we observed (each 16 seconds) an increase of the voltage which is due to the MPPT process of the PMU. In fact, the PMU opens the input periodically to buffer the input voltage and optimize its performance.

The discharge lasts several seconds where 0.25 seconds are dedicated to system initialization and 1.16 seconds to LoRaWAN transmission, as represented in Fig. 15. The remaining DC energy (deep sleep mode) could also be used for complementary measurement or a more complex computing process. The receiving of valid frames is validated on TheThingsNetwork, as shown in Fig. 9.

Although the EIRP used in these outdoor experiments were similar to the EIRP used in the anechoic chamber, the voltages at the output of the rectifier are higher and consequently the durations between charges are smaller. We can explain these advantageous results by the real power densities that are more important than the computed/estimated ones, thanks to multipath effects and the use of a wideband rectenna which can harvest energy from GSM communications in contiguous bands.



FIGURE 13. Photograph of our experimental outdoor setup (SN powered by using a WPT technique).

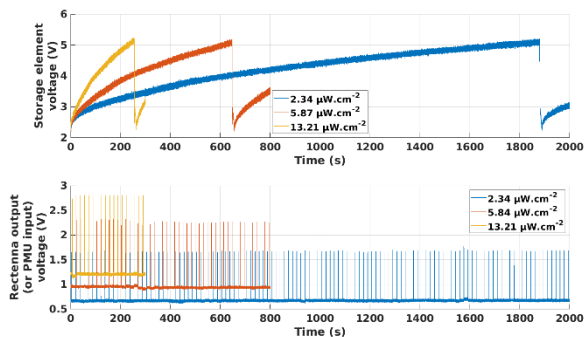


FIGURE 14. a) Voltage waveforms of the charge and discharge graphs measured at the output ports of the energy storage element (30mF) in outdoor experiments for three different generated power densities. b) Rectenna output voltage corresponding of the charge and discharge graphs.

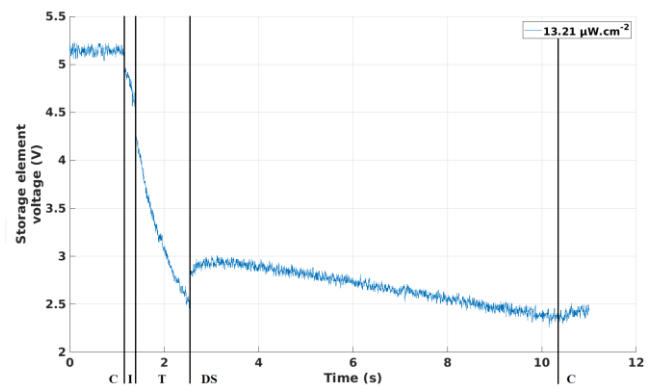


FIGURE 15. Discharge graph of the energy stored in the storage element (30mF) during the outdoor experiments. I: initialization; T: LoRa Transmission; DS: Deep Sleep mode; C: charge.

V. DISCUSSIONS

The prototype of the sensing node has been designed as a proof of the main concepts introduced in this paper: (i) the smart-node wireless network, (ii) the autonomy in energy (of the SNs) obtained by using a wireless power transmission technique, (iii) the control of the functionality of the SNs by a well-tailored wireless power transfer. The prototype of our SN operates in ISM 868 MHz frequency band (EU), receives energy from a dedicated RF source and sends data over the air by using a LoRaWAN standard. We use orthogonal polarization (vertical versus horizontal) between the WPT and data signals/waves and no jamming between WPT and data were experienced during our experiments. As long as the rectenna (used as WPT interface at SN level) is illuminated with an incoming power density higher than $1.12\mu\text{W}/\text{cm}^2$ we can perform measurements and send data with a periodicity (defined as the time elapsed between two consecutive LoRaWAN transmission that is equivalent to the inter-discharges duration of storage element) of 3 hours or lower. This periodicity can be controlled by controlling the power density illuminating the SN. Moreover, the proposed SN prototype can be switched on (cold start-up) and switched off by the WPT interface. Supposing that the EIRP of the RF source is limited at +33dBm (as imposed by ETSI regulation for an interrogator in the 868MHz ISM band [40]) we have a maximum theoretical range (free space and line of sight wave propagation) of 4 meters approximately.

Our SN prototype will evolve in order to be more complete, efficient, compact and relevant for the targeted application.

The choice of LoRaWAN technology is not definitive and was justified mainly by the availability of the infrastructure in our laboratory and by its relatively low power consumption in the transmit (Tx) mode. In order to minimize the consumption of the LoRaWAN module more, we could further optimize the software initialization and transmission processes, and eventually change the LoRa configurations (e.g. bandwidth, spreading factor, etc.) according to gateway specifications.

Among the technologies introduced in Table I, BLE is a potential alternative (to be tested in the future), that is more suitable for implementing a unidirectional uplink (Tx only) communication in a low range and low power consumption context. RuBee could also be an applicable alternative (if modules arrive on the market) because the reinforced concrete seems to be transparent at this frequency.

Regarding the energy management aspect, we must implement some improvements in order to optimize efficiency and limit losses. For our application, we have to design a specific rectenna with a well-defined useful frequency band, and a well-adapted matching between the rectifier and the PMU. The use of a unique antenna -both for the WPT and the communications- could allow a high gain of compactness. Also, the design of a specific PMU could be another way to increase the efficiency of the energy management of our system. An accurate estimation of the needed power could allow for decreased energy storage capacitance, allowing a more compact system that needs less input RF power to be completely charged. The choice of a storage element with fewer current losses would allow a gain in terms of efficiency. Another possibility is to add a low-consumption voltage regulator at the PMU output in order to have a constant voltage to supply the load. It could minimize the consumption of the LoRaWAN module because the higher the input voltage, the higher the consumption current. Finally, we must notice that the oscilloscope measurements induce losses. Indeed, the input impedance of the oscilloscope is $1M\Omega$. That says: for a measured voltage of 5.15V, a power of $26.5\mu W$ are lost and $6.0\mu W$ for 2.45V.

An optimal solution -compact and low consumption- could be developed using ASIC technology. This would have to combine a PMU, an input ADC for the measurements, an RF output from a communication module, and a logical circuit interface between input and output (to compute the measured data, and encapsulate it in a frame respecting the defined protocol).

The next step in our development is to add a sensor to have a dynamic data to transmit. Temperature and humidity are a good starting point due to their relative simplicity and low power consumption. The corrosion, detection and location of cracks is extremely pertinent information for precast reinforced concrete structure. However, corrosion requires a lot of energy and periodic calibration and detection necessitates a high quantity of data, all of which involve power hungry signal processing algorithms.

In the future, SNs will have to integrate into precast reinforced concrete elements. There are more than 1200 different methods of creating reinforced concrete, each with specific mechanical and electromagnetic properties. It is very difficult to estimate these electromagnetic properties which are never taken into consideration in the manufacturing process. However, concrete is a heterogeneous material with an electrical permittivity and a loss tangent which impacts highly the propagation of the electromagnetic waves within

it. On average, the dielectric constant -or relative permittivity- is between 4 and 8, and the delta tangent near 1, but both are highly dependant on the water concentration and the frequency of the electromagnetic wave. Thus it would be relevant to characterize the targeted reinforced concrete (e.g. by using an open-ended coaxial probe [41]). Moreover, the reinforcing elements forming the reinforced concrete could induce different behaviours: they can act as a Faraday cage, or as reflectors, according to their composition (e.g. steel, etc.), geometry, width, or spacing according to the frequency used by the communication technology.

V. CONCLUSION

A wireless network architecture was proposed for SHM applications of buildings and civil engineering structures. It consists of a meshed grid composed of batteryless sensing nodes and communicating nodes. Sensing nodes need to be integrated into concrete for implementing the innovative concept of communicating concrete as a step toward the new generation of structural monitoring systems. The architecture of the sensing node is simplified and tuned in order to minimize its power consumption. The energy autonomy of the sensing node is implemented through a dedicated WPT interface. An innovative concept is proposed here and validated by experiments: the sensing node functionality is controlled through the WPT link. By using this WPT link, the communicating nodes can switch on/switch off the sensing nodes and control wirelessly the periodicity of the measurements and the periodicity of the transmission of data.

ACKNOWLEDGMENT

We acknowledge also the help of Dr. Abderrahim Okba from LAAS CNRS Toulouse for developing the rectenna structures integrated into the WPT interface of SN.

REFERENCES

- [1]. "What is BIM?", available online at: <https://www.autodesk.com/solutions/bim>
- [2]. S. Kubler, W. Derigent, A. Thomas, and E. Rondeau, "Problem definition methodology for the 'Communicating Material' paradigm", IFAC Proceedings Volumes, vol. 43, no. 4, pp. 198–203, 2010.
- [3]. "McBIM research project", available online at http://www.agence-nationale-recherche.fr/en/anr-funded-project/?tx_lwmsuivibilan_pi2%5BCODE%5D=ANR-17-CE10-0014
- [4]. J. Jover, "Contribution à la réduction des pertes d'informations dans l'industrie du bois: utilisation de la Résonance Quadrupolaire Nucléaire pour l'identification de marqueurs chimiques et de la virtualisation du processus de production pour la détermination de nomenclatures divergentes", PhD dissertation. Université de Lorraine, 2013.
- [5]. S. Kubler, W. Derigent, A. Thomas, and E. Rondeau, "Prototyping of a communicating textile", International Conference on Industrial Engineering and Systems Management, IESM 2011, 2011.
- [6]. S. Johann, C. Strangfeld, M. Müller, B. Mieller, and M. Bartholmai, "RFID sensor systems embedded in concrete—requirements for long-term operation", Materials Today: Proceedings, vol. 4, no. 5, pp. 5827–5832, 2016.

- [7]. M. L. Wilson, and S. H. Kosmatka, "Design and control of concrete mixtures", *High-Performance Concrete*, vol. 15, p. 299, 2011.
- [8]. N. Barroca, L. M. Borges, F. J. Velez, F. Monteiro, M. Górski, and J. Castro-Gomes, "Wireless sensor networks for temperature and humidity monitoring within concrete structures", *Construction and Building Materials*, vol. 40, pp. 1156-1166, 2013.
- [9]. J. Ikonen, A. Knutas, H. Hämäläinen, M. Itonen, J. Porras, and T. Kallonen, "Use of embedded RFID tags in concrete element supply chains", *Journal of Information Technology in Construction (ITcon)*, vol. 18, no. 7, pp. 119-147, 2013.
- [10]. S. Alahakoon, D. M. Preethichandra, and E. M. Ekanayake, "Sensor network applications in structures—a survey", *EJSE Special Issue: Sensor Network on Building Monitoring: From Theory to Real Application*, pp. 1-10, 2009.
- [11]. J. W. Matiko, N. J. Grabham, S. P. Beeby, and M. J. Tudor, "Review of the application of energy harvesting in buildings", *Measurement Science and Technology*, vol. 25, no. 1, pp. 012002, 2013.
- [12]. A. Costanzo and D. Masotti, "Smart Solutions in Smart Spaces: Getting the Most from Far-Field Wireless Power Transfer", *IEEE Microw. Mag.*, vol. 17, no. 5, pp. 30-45, May 2016.
- [13]. D. Kim, A. Abu-Siada, and A. Sutinjo, "State-of-the-art literature review of WPT: Current limitations and solutions on IPT", *Electric Power Systems Research*, vol. 154, pp. 493-502, 2018.
- [14]. L. Gallucci, C. Menna, L. Angrisani, D. Asprone, R. S. L. Moriello, F. Bonavolontà, and F. Fabbrocino, "An Embedded Wireless Sensor Network with Wireless Power Transmission Capability for the Structural Health Monitoring of Reinforced Concrete Structures", *Sensors*, vol. 17, no. 11, pp. 2566, 2017.
- [15]. Y. Jang, J. K. Han, J. I. Baek, G. W. Moon, J. M. Kim, and H. Sohn, Jang, Yujin, et al. "Novel multi-coil resonator design for wireless power transfer through reinforced concrete structure with rebar array", *Future Energy Electronics Conference and ECCE Asia (IFEEC 2017-ECCE Asia)*, 2017 IEEE 3rd International. IEEE, pp. 2238-2243, 2017.
- [16]. O. Jonah, and S. V. Georgakopoulos, "Wireless power transfer in concrete via strongly coupled magnetic resonance", *IEEE Transactions on Antennas and Propagation*, vol. 61, no. 3, pp. 1378-1384, 2013.
- [17]. A. Okba, A. Takacs, H. Aubert, "900MHz Miniaturized rectenna", *IEEE MTT-S Wireless Power Transfer Conference*, Montreal, Canada, 3-7 June 2018.
- [18]. A. Okba, A. Takacs, and H. Aubert, "Compact Flat Dipole Rectenna for IoT Applications," *Progress In Electromagnetics Research C*, Vol. 87, 39-49, 2018.
- [19]. "Linear Technology - LTC3105 - 400mA Step-Up DC/DC Converter with Maximum Power Point Control and 250mV Start-Up", available online at: <https://www.analog.com/media/en/technical-documentation/data-sheets/3105fb.pdf>
- [20]. "Linear Technology - LTC3108 - Ultralow Voltage Step-Up Converter and Power Manager", available online at: <https://www.analog.com/media/en/technical-documentation/data-sheets/3108fc.pdf>
- [21]. "Texas Instruments - bq25504 Ultra Low-Power Boost Converter With Battery Management for Energy Harvester Applications", available online at: <http://www.ti.com/lit/ds/symlink/bq25504.pdf>
- [22]. Nippon Chemi-Con - Miniature Aluminum Electrolytic capacitors - LBK Series", available online at: http://www.chemi-con.co.jp/cgi-bin/CAT_DB/SEARCH/cat_db_al.cgi?e=e&j=p&pdfname=lbk
- [23]. "AVX BestCap® Ultra-low ESR High Power Pulse Supercapacitors", available online at: <http://datasheets.avx.com/BestCap.pdf>
- [24]. "Kemet - Supercapacitors - FM Series", available online at: https://content.kemet.com/datasheets/KEM_S6012_FM.pdf
- [25]. "STMicroelectronics - B-L072Z-LRWAN1", available online at: <https://www.st.com/en/evaluation-tools/b-l072z-lrwan1.html>
- [26]. "Murata: LoRa Module Data Sheet", available online at: https://wireless.murata.com/RFM/data/type_abz.pdf
- [27]. "STMicroelectronics - STM32L072x8 STM32L072xB STM32L072xZ", available online at: <https://www.st.com/resource/en/datasheet/stm32l072v8.pdf>
- [28]. "Semtech - LoRa - SX1276/77/78/79", available online at: <https://www.semtech.com/products/wireless-rf/lora-transceivers/SX1276>
- [29]. "The Things Network", available online at: <https://www.thethingsnetwork.org/>
- [30]. LoRa Alliance Technical Committee, "LoRaWAN 1.1 specification", 2017.
- [31]. IEEE 802.15.1 Working Group, "IEEE Standard for information technology - Telecommunications and information exchange between systems - Local and metropolitan area networks - Specific requirements - Part 15.1: Wireless Medium Access Control (MAC) and Physical layer (PHY) specifications for Wireless Personal Area Networks (WPANs)", IEEE Std 802.15.1, 2005.
- [32]. IEEE 802.15.3 Working Group, "IEEE Standard for high data rate wireless multi-media networks", IEEE Std 802.15.3, 2016.
- [33]. IEEE 802.15.4 Working Group, "IEEE Standard for local area metropolitan area networks - Part 15.4: Low-rate Wireless Personal Area Networks (LR-WPANs)", IEEE Std 802.15.4, 2011.
- [34]. IEEE 802.11 Working Group, "IEEE Standard for information technology - Telecommunications and information exchange between systems - Local and metropolitan area networks - Specific requirements - Part 11: Wireless LAN Medium Access Control (MAC) and Physical layer (PHY) specifications", IEEE Std 802.11, 2007.
- [35]. IEEE 1902.1 Working Group, "IEEE Standard for long wavelength wireless network protocol", IEEE Std 1902.1, 2009.
- [36]. "NXP: QN908x: Ultra low power Bluetooth 5 system-on-chip solution", available online at: <https://www.nxp.com/docs/en/nxp/data-sheets/QN908x.pdf>
- [37]. "decaWave: DWM1000", available online at: <https://www.decawave.com/sites/default/files/resources/DWM1000-Datasheet-V1.6.pdf>
- [38]. "Atmel: ZIGBIT 900MHZ WIRELESS MODULES", available online at: http://ww1.microchip.com/downloads/en/DeviceDoc/atmel-42269-wireless-zigbit-atz-rf-212b-0-cn_datasheet.pdf
- [39]. "Silicon Labs: Zentri AMW036/AMW136", available online at: <https://www.silabs.com/documents/login/data-sheets/ADS-MWx36-ZentriOS-101R.pdf>
- [40]. ETSI, "Electromagnetic compatibility and Radio spectrum Matters (ERM); Short Range Devices (SRD) intended for operation in the bands 865 MHz to 868 MHz and 915 MHz to 921 MHz; Guidelines for the installation and commissioning of Radio Frequency Identification (RFID) equipment at UHF", ETSI TR 102 436, V2.1.1", 2014.
- [41]. B. Filali, F. Boone, J. Rhazi, and G. Ballivy, "Design and calibration of a large open-ended coaxial probe for the measurement of the dielectric properties of concrete", *IEEE Transactions on Microwave Theory and Techniques*, vol. 56, no. 10, pp. 2322-2328, 2008.

Gaël Loubet was born in Toulouse, France, in February 1994. He received the Engineering diploma in electronics and automation engineering from the *National Institute of Applied Sciences (INSA)*, Toulouse, France, in July 2017. He is currently pursuing a Ph.D. degree in micro- and nano-systems for communications at the *National Institute of Applied Sciences (INSA)*, Toulouse, France. His research interests include communicating materials paradigm, electromagnetic wireless power transfer, wireless communication for internet of things applications and wireless sensor networks for structural health monitoring applications.

Alexandru Takacs (M'12) was born in Simleu Silvaniei, Romania, in March 1975. He received the Engineer diploma in electronic engineering from the Military Technical Academy, Bucharest, Romania, in 1999, and the Master degree and Ph.D. degree in microwave and optical communications from the National Polytechnic Institute of Toulouse (INPT), Toulouse, France, in 2000 and 2004, respectively. From 2004 to 2007, he was a Lecturer with the Military Technical Academy of Bucharest, and an Associate Researcher with the Microtechnology Institute of Bucharest. From 2008 to 2010, he occupied a Postdoctoral position with the Laboratory for Analysis and Architecture of Systems (LAAS), National Center for Scientific Research (CNRS), Toulouse, France. During 2011, he was an R&D RF Engineer with Continental Automotive SAS France, where he was in charge of antenna design and automotive electromagnetic simulation. Since 2012, he has been an Associate Professor with the University (Paul Sabatier), Toulouse, France, where he performs research within LAAS-CNRS. He has authored or coauthored one book, one book chapter, 15 papers in refereed journals, and over 70 communications in international symposium proceedings. His research interests include the design of microwave and RF circuits, energy harvesting and wireless power transfer, microelectromechanical systems (MEMS) circuits and systems, small antenna design, electromagnetic simulation techniques, and optimization methods.

Daniela Dragomirescu (M'96-SM'15) Daniela Dragomirescu is Professor at the University of Toulouse (INSA Toulouse) and LAAS-CNRS laboratory. She received the engineering degree with Magna Cum Laude from the Polytechnic University of Bucarest, Romania in 1996, the MSc in circuits design from the University Paul Sabatier, France, in 1997 and the Ph.D. degree with Magna Cum Laude in 2001 from the University of Toulouse, France. Prof. Dragomirescu is the Head of Microwave and Photonics Systems Department, in LAAS-CNRS laboratory since January 2015. She is the IEEE Solid States Circuits French Chapter Chair. Prof. Daniela Dragomirescu was French Government Fellow of Churchill College, University of Cambridge from February to September 2014. Daniela Dragomirescu is the Dean of Electrical and Computer Engineering Department at INSA Toulouse since June 2017. Prof. Dragomirescu is conducting research in the area of wireless communications with a special focus on Wireless Sensor Networks. Daniela Dragomirescu received in 2005 the French National Research Agency grant for Young Investigator which supported her in setting up the team in the Wireless Sensor Network area. She was also involved in many national and European research projects in the area of wireless communication. Daniela Dragomirescu was the coordinator of one of the nine French NanoInnov project, called Nanocomm on Reconfigurable wireless nano-sensors networks. She published more than 80 papers in journals and conferences proceedings, 2 patents and she authored 7 academic courses.

TABLE I
COMPARATIVE STUDY OF WIRELESS COMMUNICATION TECHNOLOGIES

Technology	Standard	Directionality	Frequency	Theoretical range	Minimal frame size (byte)	Module	Manufacturer	Transmission / Reception power consumption (mW)
LoRa	LoRaWAN [30]	'Transmission only' possible	433/868/915MHz (ISM)	Several kilometers	14	CMWX1ZZABZ-091 [26]	Murata	119 at +10dBm (typ) / Not necessary
Bluetooth LowEnergy (BLE)	IEEE 802.15.1 [31]	'Transmission only' possible / Essentially bidirectional	2.4GHz (ISM)	Thousands meters	11	QN908x [36]	NXP	12 at 0dBm (typ) / 12 at 1Mbps (typ)
Ultra-Wide Band (UWB)	IEEE 802.15.3 [32]	Essentially bidirectional	3.1-10.6GHz	Tens meters	N/A	DWM1000 [37]	DecaWave	462 at +9.3dBm (max) / 528 (max)
ZigBee	IEEE 802.15.4 [33]	Bidirectional	868/915MHz 2.4GHz (ISM)	Thousand meters	16	ATZB-RF-212B-0-CN [38]	Atmel	17 at +9dBm (typ) / 31 (typ)
Wi-Fi	IEEE 802.11 [34]	Bidirectional	900MHz 2.4GHz 5GHz (ISM)	Tens meters	33	Zentri AMWx36 [39]	Silicon Labs	19 at 1Mbps (typ)
RuBee	IEEE 1902.1 [35]	Essentially bidirectional	131kHz	30 meters	5	N/A	N/A	N/A / N/A

The power is computed for a 3.3V supply (except for Bluetooth Low Energy and ZigBee modules and their 3V supply). We have to take into consideration the duration of a transmission and reception, and the quantity of needed control frames to estimate precisely the consumption for each standard and module.

TABLE II
CHARACTERISTICS OF THE SN PROTOTYPE FOR DIFFERENT USE CASES

Energy storage element	Rectifier input power (dBm)	Rectifier open-load output voltage (V)	Nominal rectifier output voltage (mV)	Maximal/ Minimal voltage at the output port of the storage element (V)	Energy stored (mJ)	Cold start duration	First charge duration	Inter-discharges duration	Discharge duration (s)
ELBK350ELL602AMN3S 6mF	-4	N/A	N/A	3.40 / 2.80	11.2	N/A	~42min	~2min29s	N/A
BZ05FB682ZSB 6.8mF	-7	N/A	N/A	3.40 / 2.80	12.6	N/A	~2h03min	~5min14s	N/A
BZ05FB682ZSB 6.8mF	-4	N/A	N/A	3.40 / 2.80	12.6	N/A	~43min	~2min20s	N/A
FM0H103ZF 10mF	-4	N/A	N/A	3.40 / 2.80	18.6	N/A	~49min	~2min23s	N/A
20mF (two FM0H103ZF of 10mF on parallel)	-4	1.25	510	5.15 / 2.80	186.8	~58min	~1h23min	~16min	~0.750
30mF (three FM0H103ZF of 10mF on parallel)	-4	1.28	500	5.15 / 2.80	280.2	~1h18min	~2h31min	~26min	~1.21
30mF (three FM0H103ZF of 10mF on parallel)	-2	1.38	575	5.15 / 2.80	280.2	~1h	~1h21min	~16min	~1.20
30mF (three FM0H103ZF of 10mF on parallel)	0	1.53	630	5.15 / 2.80	280.2	~42min	~1h08min	~11min	~1.25
30mF (three FM0H103ZF of 10mF on parallel)	2	1.76	740	5.15 / 2.80	280.2	~32min	~48min	~7min	~1.20
30mF (three FM0H103ZF of 10mF on parallel)	4	1.99	760	5.15 / 2.80	280.2	~18min	~28min	~5min	~1.36
30mF (three FM0H103ZF of 10mF on parallel)	6	2.06	860	5.15 / 2.80	280.2	~10min	~16min	~3min	~1.42
30mF (three FM0H103ZF of 10mF on parallel)	8	2.20	900	5.15 / 2.80	280.2	~4min35s	~9min20s	~2min	~1.49
30mF (three FM0H103ZF of 10mF on parallel)	10	2.34	1000	5.15 / 2.80	280.2	~1min45s	~5min22s	~1min09s	~1.48

A rectifier is connected directly to an Anritsu MG3694B power synthesizer. The PMU (bq25504, Texas Instruments) is connected as load for the rectifier. PMU charges various combinations of supercapacitors. The energy stored in these supercapacitors is used to power a LoRaWAN module. The voltage measurements are performed by using a LeCroy WaveRunner 6100 oscilloscope. The cold start voltage (provided by the rectifier) required to switch on the PMU is around 350mV.

TABLE III
 CHARACTERISTICS OF THE SN PROTOTYPE FOR A COMPLETE WPT IN AN ANECHOIC CHAMBER

EIRP (dBm)	Power density ($\mu\text{W}/\text{cm}^2$) [computation]	Rectenna input power (dBm) [computation]	Nominal rectifier output voltage (mV)	Inter-discharges duration	Discharge duration (s)
26.7	1.65	-5.8	514	~1h32min	~9.0
27.7	2.08	-4.8	557	~1h00min	~8.9
28.7	2.62	-3.8	626	~42min22s	~8.9
29.7	3.30	-2.8	705	~29min12s	~8.9
30.7	4.16	-1.8	791	~19min41s	~8.9

A power transmitter composed of a power synthesizer (Anritsu MG3694B, operating at 868MHz) and a patch antenna with +9.2dBi of gain is used as power source for generating the electromagnetic power density that illuminates the prototype under test. The total losses of the cable and connectors used to interconnect the power generator with patch antenna are approximately -2.5dB. The measurements were performed in an anechoic chamber to avoid any interference or multipath effect. The prototype is composed of: a 3D rectenna (the rectenna's antenna gain is around +2.2dBi at 868MHz), the PMU bq25504 connected to a supercapacitors array of 30mF, as well as the LoRaWAN module B-L072Z-LRWAN1. The distance between the power transmitter and the rectenna is 150cm. The voltage measurements are performed by using a LeCroy WaveRunner 6100 oscilloscope. The cold start voltage (provided by the rectenna) required to switch on the PMU is around 350mV. Start and stop thresholds for the discharge are configured at 5.15V and 2.45V respectively. The duration of our processing in the SN is around 1.4s.

TABLE IV
CHARACTERISTICS OF THE PROTOTYPE FOR A COMPLETE WPT OUTDOORS

EIRP (dBm) / Distance (cm))	Power density ($\mu\text{W}/\text{cm}^2$) [computation]	Rectenna input power (dBm) [computation]	Nominal rectifier output voltage (mV)	Inter-discharges duration	Discharge duration (s)
25.0 / 150	1.12	-7.4	490	~2h59min	8.8
28.2 / 150	2.34	-4.3	688	~31min28s	8.8
30.2 / 150	3.70	-2.3	816	~18min26s	9.2
32.2 / 150	5.87	-0.3	964	~10min56s	9.5
31.2 / 100	10.49	+2.2	1179	~5min13s	8.9
32.2 / 100	13.21	+3.2	1231	~4min24s	9.3

A power transmitter composed of a power synthesizer (Anritsu MG3694B, operating at 868MHz) and a patch antenna with +9.2dBi of gain is used as power source for generating the electromagnetic power density that illuminates the prototype under test. The total losses of the cable and connectors used to interconnect the power generator with patch antenna are approximately -1 dB. The measurements were performed in a balcony of our laboratory in order to make easier the LoRaWAN communication. The prototype is composed of: a 3D rectenna (the rectenna's antenna gain is around +2.2dBi at 868MHz), the PMU bq25504 connected to a supercapacitors array of 30mF, as well as the LoRaWAN module B-L072Z-LRWAN1. The voltage measurements are performed by using a LeCroy WaveRunner 6100 oscilloscope. The cold start voltage (provided by the rectenna) required to switch on the PMU is around 350mV. Start and stop thresholds for the discharge are configured at 5.15V and 2.45V respectively. The LoRaWAN transmission lasts nearly 1.16s, and the initialization of the system 0.24s, that says a 1.4s period for our processing. The polarization of the power transmission and LoRaWAN communication are orthogonal in order to avoid eventual interferences.